Inorg. Chem. **2002**, *41*, 2400–2407

Low-Temperature UV–Visible and NMR Spectroscopic Investigations of O_2 Binding to (^{6}L)Fe^{II}, a Ferrous Heme Bearing Covalently Tethered Axial Pyridine Ligands

Reza A. Ghiladi and Kenneth D. Karlin*

Department of Chemistry, The Johns Hopkins University, Charles and 34th Streets, Baltimore, Maryland 21218

Received April 2, 2001

In this report, we describe the reversible dioxygen reactivity of (^{6}L)Fe^{II} (**1**) {^{6}L = partially fluorinated tetraphenylporphyrin with covalently appended TMPA moiety; TMPA = tris(2-pyridylmethyl)amine} using a combination of low-temperature UV–vis and multinuclear (^{1}H and ^{2}H) NMR spectroscopies. Complex **1**, or its pyrrole-deuterated analogue (^{6}L-d_8)Fe^{II} (**1-d_8**), exhibits downfield shifted pyrrole resonances (δ 28–60 ppm) in all solvents utilized {CH_2Cl_2, $(CH_3)_2C(O)$, CH_3CN, THF}, indicative of a five-coordinate high-spin ferrous heme, even when there is no exogenous axial solvent ligand present (i.e., in methylene chloride). Furthermore, (^{6}L)Fe^{II} (**1**) exhibits non-pyrrolic upfield and downfield shifted peaks in CH_2Cl_2, $(CH_3)_2C(O)$, and CH_3CN solvents, which we ascribed to resonances arising from the intra- or intermolecular binding of a TMPA–pyridyl arm to the ferrous heme. Upon exposure to dioxygen at 193 K in methylene chloride, (^{6}L)Fe^{II} (**1**) {UV–vis: λ_{max} = 433 (Soret), 529 (sh), 559 nm} reversibly forms a dioxygen adduct {UV–vis: λ_{max} = 422 (Soret), 542 nm}, formulated as the six-coordinate low-spin {$\delta_{pyrrole}$ 9.3 ppm, 193 K} heme–superoxo complex (^{6}L)Fe^{III}–(O_2^-) (**2**). The coordination of the tethered pyridyl arm to the heme–superoxo complex as axial base ligand is suggested. In coordinating solvents such as THF, reversible oxygenation (193 K) of (^{6}L)Fe^{II} (**1**) {UV–vis: λ_{max} = 424 (Soret), 542 nm} also occurs to give a similar adduct (^{6}L)Fe^{III}–(O_2^-) (**2**) {UV–vis: λ_{max} = 418 (Soret), 537 nm. ^{2}H NMR: $\delta_{pyrrole}$ 8.9 ppm, 193 K}. Here, we are unable to distinguish between a bound solvent ligand or tethered pyridyl arm as axial base ligand. In all solvents, the dioxygen adducts decompose (thermally) to the ferric–hydroxy complex (^{6}L)Fe^{III}–OH (**3**) {UV–vis: λ_{max} = 412–414 (Soret), 566–575 nm; $\sim\delta_{pyrrole}$ 120 ppm at 193 K}. This study on the O_2-binding chemistry of the heme-only homonuclear (^{6}L)Fe^{II} (**1**) system lays the foundation for a more complete understanding of the dioxygen reactivity of heterobinuclear heme–Cu complexes, such as [(^{6}L)Fe^{II}Cu^I]$^+$, which are models for cytochrome *c* oxidase.

Introduction

In light of the importance and essential nature of dioxygen transport and storage by hemoglobin and myoglobin, investigations into the reactivity of synthetic heme−iron(II) complexes with O_2 have unceasingly and deservedly attracted much attention.[1−8] A resurgence of interest into heme−O_2 chemistry has also been ignited by the recent studies on heme proteins which sense small molecules such as O_2, CO, and NO; for example, FixL is a dioxygen-sensing heme protein which is thought to mediate biological processes (i.e., transcription and regulation).[9,10] Such inquiries also bear upon dioxygen activation chemistry,[11−15] such as that occurring in the cytochrome P-450 monooxygenase enzymes.[11,12,16]

Our own interests in this area come from a combination of heme and copper dioxygen chemistry, as is important at the active site of cytochrome *c* oxidase and other heme−

* To whom correspondence should be addressed. E-mail: karlin@jhu.edu.

(1) Momenteau, M.; Reed, C. A. *Chem. Rev.* **1994**, *94*, 659−698.
(2) Traylor, T. G.; Traylor, P. S. In *Active Oxygen: Active Oxygen in Biochemistry*; Valentine, J. S., Foote, C. S., Greenberg, A., Liebman, J. F., Eds.; Chapman and Hall: New York, 1995; pp 84−187.
(3) Bakac, A. *Prog. Inorg. Chem.* **1995**, *43*, 267−351.
(4) Collman, J. P.; Halbert, T. R.; Suslick, K. S. In *Metal Ion Activation of Dioxygen*; T. G. Spiro, Ed.; John Wiley and Sons: New York, 1980; pp 1−72.
(5) Collman, J. P. *Inorg. Chem.* **1997**, *36*, 5145−5155.
(6) Collman, J. P.; Eberspacher, T.; Fu, L.; Herrmann, P. C. *J. Mol. Catal. A: Chem.* **1997**, *117*, 9−20.
(7) Collman, J. P.; Fu, L. *Acc. Chem. Res.* **1999**, *32*, 455−463.
(8) Perutz, M. F. *Annu. Rev. Physiol.* **1990**, *52*, 1−25.
(9) Chan, M. K. *Curr. Opin. Chem. Biol.*, in press.
(10) Rodgers, K. R. *Curr. Opin. Chem. Biol.* **1999**, *3*, 158−167.

10.1021/ic0103547 CCC: $22.00
Published on Web 04/03/2002

copper oxidase proton pumps. Recent biochemical and notable protein X-ray structural advances[17−22] reveal that O_2-binding and reduction occurs at an active site consisting of a high-spin heme group (with proximal histidine), which lies at ∼4.5 Å from Cu_B, which possesses three histidine nitrogen ligands. While an initial O_2-interaction with Cu_B is postulated,[23,24] the latest emerging picture is that the metal−O_2 chemistry is dominated by the heme, with Cu_B being critical for electron transfer and proton-translocation chemistry.[19,21,25−27] Our research program is focused upon elucidating the fundamental aspects of O_2-interactions with heme and copper centers found either in close proximity, or even just in combination.

To these ends, we have been studying the dioxygen reactivity of 1:1 mixtures of the porphyrinate−iron(II) complex (F_8TPP)Fe^{II} (Chart 1; Ar^F = 2,6-difluorophenyl) with copper(I) complexes, either [(TMPA)Cu^I(MeCN)]$^+$ (TMPA = tris(2-pyridylmethyl)amine) or [(MePY2)Cu^I(MeCN)]$^+$ (MePY2 = *N*,*N*-bis[2-(2-pyridyl)ethyl]methylamine).[28−32] Additional efforts have focused on their analogous binucleating ligand systems, ^{6}L and ^{4}L, wherein a tetradentate (TMPA in the case of [(^{6}L)Fe^{II}Cu^I]$^+$)[33] or tridentate (MePY2, as in [(^{4}L)Fe^{II}Cu^I]$^+$)[34] copper chelate is covalently appended to the periphery of a 2,6-difluorophenyl substituted porphyrin. For all cases, early studies of O_2-reactivity with these Fe^{II}−Cu^I complexes reveal the presence of interesting O_2-intermediates (Chart 1), detected either by low-temperature spectral studies or stopped-flow spectrophotometry. Notably, in the case of the tetradentate system [(^{6}L)Fe^{II}Cu^I]$^+$, a unique high-spin heme−copper peroxo complex, [(^{6}L)Fe^{III}−(O_2^{2-})−Cu^{II}]$^+$,[33] has been extensively characterized, with a similar μ-peroxo species formed in the untethered analogue, [(F_8TPP)Fe^{III}−(O_2^{2-})−Cu^{II}(TMPA)]$^+$.[35] Similar observations of O_2-intermediates, including heme−peroxo−Cu species, are seen when tridendate copper chelates are employed, as for (F_8TPP)Fe^{II}/[(MePY2)Cu^I(MeCN)]$^+$ [32] and its tethered analogue [(^{4}L)Fe^{II}Cu^I]$^+$.[34]

Our previous studies on the copper(I)/O_2 chemistry of [(TMPA)Cu^I(MeCN)]$^+$ [36,37] and [(MePY2)Cu^I(MeCN)]$^+$ [38,39] provide us with a considerable understanding of the O_2-complexes involved in these copper-only systems. However, to fully understand the nature of synthetic heme−copper/O_2 reactions described previously, we need to also fully

Chart 1

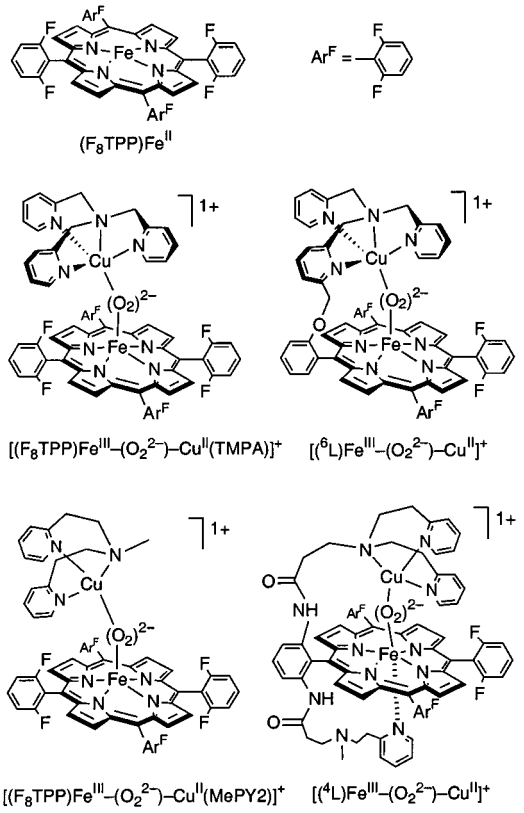

(11) Sono, M.; Roach, M. P.; Coulter, E. D.; Dawson, J. H. *Chem. Rev.* **1996**, *96*, 2841−2887.
(12) Ortiz de Montellano, P. R. *Cytochrome P-450: Structure, Mechanism and Biochemistry.*, 2nd ed.; Plenum: New York, 1995.
(13) Valentine, J. S.; Wertz, D. L.; Lyons, T. J.; Liou, L.-L.; Goto, J. J.; Gralla, E. B. *Curr. Opin. Chem. Biol.* **1998**, *2*, 253−262.
(14) Sisemore, M. F.; Selke, M.; Burstyn, J. N.; Valentine, J. S. *Inorg. Chem.* **1997**, *36*, 979−984.
(15) *Active Oxygen in Biochemistry*; Valentine, J. S., Foote, C. S., Greenberg, A., Liebman, J. F., Eds.; Chapman and Hall: New York, 1995.
(16) Schlichting, I.; Berendzen, J.; Chu, K.; Stock, A. M.; Maves, S. A.; Benson, D. E.; Sweet, B. M.; Ringe, D.; Petsko, G. A.; Sligar, S. G. *Science* **2000**, *287*, 1615−1622.
(17) Yoshikawa, S.; Shinzawa-Itoh, K.; Nakashima, R.; Yaono, R.; Yamashita, E.; Inoue, N.; Yao, M.; Jei-Fei, M.; Libeu, C. P.; Mizushima, T.; Yamaguchi, H.; Tomizaki, T.; Tsukihara, T. *Science* **1998**, *280*, 1723−1729.
(18) Ostermeier, C.; Harrenga, A.; Ermler, U.; Michel, H. *Proc. Natl. Acad. Sci. U.S.A.* **1997**, *94*, 10547−10553.
(19) Babcock, G. T. *Proc. Natl. Acad. Sci. U.S.A.* **1999**, *96*, 12971−12973.
(20) Ferguson-Miller, S.; Babcock, G. T. *Chem. Rev.* **1996**, *96*, 2889−2907.
(21) Gennis, R. B. *Proc. Natl. Acad. Sci. U.S.A.* **1998**, *95*, 12747−12749.
(22) Michel, H.; Behr, J.; Harrenga, A.; Kannt, A. *Annu. Rev. Biophys. Biomol. Struct.* **1998**, *27*, 329−356.
(23) Oliveberg, M.; Malmström, B. G. *Biochemistry* **1992**, *31*, 3560−3563.
(24) Blackmore, R. S.; Greenwood, C.; Gibson, Q. H. *J. Biol. Chem.* **1991**, *266*, 19245−19249.
(25) Michel, H. *Proc. Natl. Acad. Sci. U.S.A.* **1998**, *95*, 12819−12824.
(26) Verkhovsky, M. I.; Jasaitis, A.; Verkhovskaya, M. L.; Morgan, J. E.; Wikström, M. *Nature* **1999**, *400*, 480−483.
(27) Wikström, M. *Biochim. Biophys. Acta* **2000**, *1458*, 188−198.
(28) Karlin, K. D.; Nanthakumar, A.; Fox, S.; Murthy, N. N.; Ravi, N.; Huynh, B. H.; Orosz, R. D.; Day, E. P. *J. Am. Chem. Soc.* **1994**, *116*, 4753−4763.
(29) Nanthakumar, A.; Fox, S.; Murthy, N. N.; Karlin, K. D.; Ravi, N.; Huynh, B. H.; Orosz, R. D.; Day, E. P.; Hagen, K. S.; Blackburn, N. J. *J. Am. Chem. Soc.* **1993**, *115*, 8513−8514.
(30) Nanthakumar, A.; Fox, S.; Karlin, K. D. *J. Chem. Soc., Chem. Commun.* **1995**, 499−501.
(31) Nanthakumar, A.; Fox, S.; Murthy, N. N.; Karlin, K. D. *J. Am. Chem. Soc.* **1997**, *119*, 3898−3906.
(32) Kopf, M.-A.; Neuhold, Y.-M.; Zuberbühler, A. D.; Karlin, K. D. *Inorg. Chem.* **1999**, *38*, 3093−3102.
(33) Ghiladi, R. A.; Ju, T. D.; Lee, D.-H.; Moënne-Loccoz, P.; Kaderli, S.; Neuhold, Y.-M.; Zuberbühler, A. D.; Woods, A. S.; Cotter, R. J.; Karlin, K. D. *J. Am. Chem. Soc.* **1999**, *121*, 9885−9886.
(34) Kopf, M.-A.; Karlin, K. D. *Inorg. Chem.* **1999**, *38*, 4922−4923.
(35) Ghiladi, R. A.; Hatwell, K. R.; Karlin, K. D.; Huang, H.-w.; Moënne-Loccoz, P.; Krebs, C.; Huynh, B. J.; Marzilli, L. A.; Cotter, R. J.; Kaderli, S.; Zuberbühler, A. D. *J. Am. Chem. Soc.* **2001**, *123*, 6183−6184.
(36) Tyeklár, Z.; Jacobson, R. R.; Wei, N.; Murthy, N. N.; Zubieta, J.; Karlin, K. D. *J. Am. Chem. Soc.* **1993**, *115*, 2677−2689.
(37) Karlin, K. D.; Kaderli, S.; Zuberbühler, A. D. *Acc. Chem. Res.* **1997**, *30*, 139−147.
(38) Liang, H.-C.; Karlin, K. D.; Dyson, R.; Kaderli, S.; Jung, B.; Zuberbühler, A. D. *Inorg. Chem.* **2000**, *39*, 5884−5894.
(39) Obias, H. V.; Lin, Y.; Murthy, N. N.; Pidcock, E.; Solomon, E. I.; Ralle, M.; Blackburn, N. J.; Neuhold, Y.-M.; Zuberbühler, A. D.; Karlin, K. D. *J. Am. Chem. Soc.* **1998**, *120*, 12960−12961.

characterize the O_2-chemistry of the synthetic heme present in our tethered heterobinuclear complexes. While we have carried out a detailed study of $(F_8TPP)Fe^{II}$ (**1**)/O_2 chemistry,[40] which expanded our knowledge of the heme/O_2 chemistry present in the untethered $[(F_8TPP)Fe^{II}/(L)Cu^{I}]^+$ {L = TMPA or MePY2} systems, it is necessary to examine the dioxygen reactivity of the copper-free (empty TMPA-tether) complex $(^6L)Fe^{II}$ (**1**) {see diagram} in order to fully deduce the O_2-binding and reduction chemistry of the tethered heme−Cu $[(^6L)Fe^{II}Cu^{I}]^+$ complex.

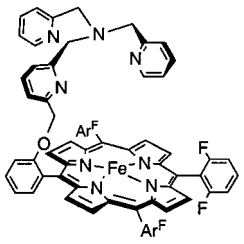

$(^6L)Fe^{II}$ (**1**)

Thus, a detailed study of $(^6L)Fe^{II}$ (**1**)/O_2 chemistry is the focus of the present report. We find that $(^6L)Fe^{II}$ (**1**) reacts with O_2 reversibly in a number of solvents, forming low-temperature stable dioxygen adducts, characterized by both UV−vis and NMR spectroscopies. Unlike its parent porphyrin complex, $(F_8TPP)Fe^{II}$, which has previously been shown to react reversibly with dioxygen to form the heme−superoxo $(F_8TPP)Fe^{III}-(O_2^-)$ and heme−peroxo−heme $(F_8TPP)Fe^{III}-(O_2^{2-})-Fe^{III}(F_8TPP)$ complexes in coordinating and noncoordinating solvents, respectively,[40] $(^6L)Fe^{II}$ (**1**) reacts with dioxygen to form predominantly the heme−superoxo complex $(^6L)Fe^{III}-(O_2^-)$ (**2**), regardless of the solvent used in the oxygenation reaction. We suggest that this observed difference in O_2 chemistry between $(^6L)Fe^{II}$ (**1**) and $(F_8TPP)Fe^{II}$ is due to the presence of the pyridyl arms (from the Cu-free TMPA tether) in complex **1**, which provide the heme with an internal axial base ligand.

Results and Discussion

Synthesis. $(^6L)Fe^{II}$ (**1**) and $(^6L\text{-}d_8)Fe^{II}$ (**1-*d*$_8$**) complexes were synthesized as described elsewhere.[41,42] By selectively deuterating the pyrrole hydrogens (up to 90 atom % D incorporation by mass spectrometric analysis), a full ^2H NMR study of the $(^6L\text{-}d_8)Fe^{II}$ (**1-*d*$_8$**) oxygenation reaction was performed, which provided unambiguous assignment of the porphyrinate pyrrole hydrogens. This proved helpful given β-pyrrole-H chemical shifts are extremely useful in the assignment of oxidation and spin state of the heme, as well as in identifying the type of dioxygen adduct formed.[43−45]

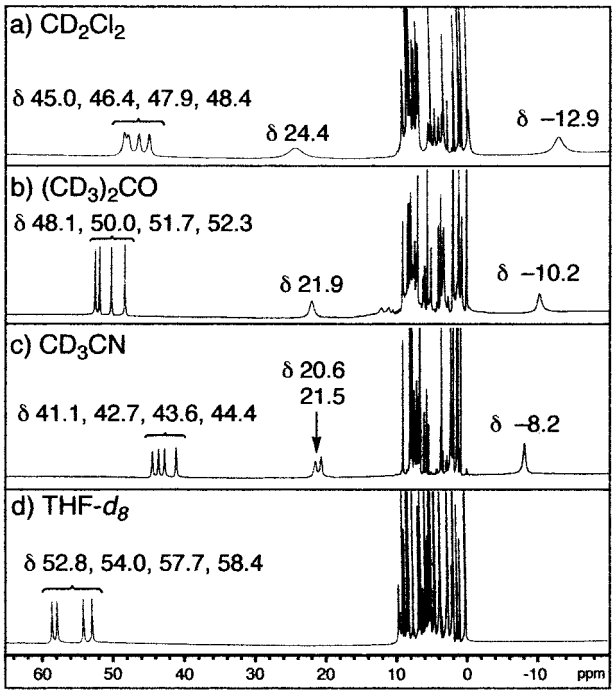

Figure 1. ^1H NMR spectra of $(^6L)Fe^{II}$ (**1**) in various solvents at room temperature.

Table 1. ^1H NMR Spectroscopic Data of the Paramagentically Shifted Resonances of $(^6L)Fe^{II}$ (**1**) and $(F_8TPP)Fe^{II}$ in Various Solvents (Room Temperature)

	$(^6L)Fe^{II}$ (**1**)		$(F_8TPP)Fe^{II}$
solvent	$\delta_{pyrrole}$ (ppm)	$\delta_{pyridyl}$ (ppm)	$\delta_{pyrrole}$ (ppm)
methylene chloride	44.96, 46.40, 47.89, 48.43	24.4, −12.9	4.9 ($S = 1$)
acetone	48.13, 50.01, 51.66, 52.28	21.9, −10.2	48 ($S = 2$)
acetonitrile	41.09, 42.72, 43.58, 44.43	20.6, 21.5, −8.2	28 (spin equilibrium)
tetrahydrofuran	52.79, 54.01, 57.66, 58.39	N/A	56 ($S = 2$)

Pyridyl Arm Coordination to the Ferrous Heme in $(^6L)Fe^{II}$ (1). ^1H NMR spectroscopy of $(^6L)Fe^{II}$ (**1**) in weakly coordinating or noncoordinating solvents revealed, in addition to the observation of paramagnetically shifted pyrrole resonances, the presence of upfield and downfield shifted resonances which we ascribe to the ferrous ion coordination of a pyridyl arm from the TMPA tether in ^6L. We arrive at this conclusion through comparisons of the ^1H NMR spectra of $(^6L)Fe^{II}$ (**1**) to those spectra of $(F_8TPP)Fe^{II}$,[40] in which no pyridyl arm is present. Marked differences are observed (Table 1 and Figure 1). First, for all solvents, the pyrrole-H resonances of $(^6L)Fe^{II}$ (**1**) are found downfield (40−60 ppm) and are split into four distinct peaks, each integrating to two protons, for a total of eight pyrrolic hydrogens observed. Splitting of the pyrrole-H resonances due to the asymmetry of the porphyrin macrocycle for tetraarylporphyrins has been

(40) Ghiladi, R. A.; Kretzer, R. M.; Guzei, I.; Rheingold, A. L.; Neuhold, Y.-M.; Hatwell, K. R.; Zuberbühler, A. D.; Karlin, K. D. *Inorg. Chem.* **2001**, *40*, 5754−5767.
(41) Ju, T. D.; Ghiladi, R. A.; Lee, D.-H.; van Strijdonck, G. P. F.; Woods, A. S.; Cotter, R. J.; Young, J., V. G.; Karlin, K. D. *Inorg. Chem.* **1999**, *38*, 2244−2245.
(42) Ghiladi, R. A.; Lee, D.-H.; Huang, H.-w.; Moënne-Loccoz, P.; Kaderli, S.; Zuberbühler, A. D.; Woods, A. S.; Cotter, R. J.; Karlin, K. D. Manuscript in preparation.
(43) Goff, H. M.; La Mar, G. N. *J. Am. Chem. Soc.* **1977**, *99*, 6599−6606.
(44) Walker, F. A.; Simonis, U. In *Biological Magnetic Resonance*; Berliner, L. J., Reuben, J., Eds.; NMR of Paramagnetic Molecules Vol. 12; Plenum Press: New York, 1993; pp 133−274.
(45) Walker, F. A. In *The Porphyrin Handbook*; Kadish, K. M., Smith, K. M., Guilard, R., Eds.; NMR and EPR Vol. 5; Academic Press: San Diego, 2000; pp 81−184.

observed previously, notably in the "picket fence" and "pocket" porphyrins of Collman and co-workers,[46,47] in the double-sided porphyrinatoiron(II) complexes of Tsuchida and co-workers,[48] in the "basket handle" porphyrins of Momenteau and co-workers,[49,50] and in the heme−Cu complex $[(^4L)Fe^{II}Cu^{I}]^+$.[34] This solvent-independent downfield-shifting of the β-pyrrole-H resonances is indicative of a consistent five-coordinate high-spin ($S = 2$) ferrous heme.[43−45]

These results for (^{6}L)Fe^{II} (**1**) contrast with those ^{1}H NMR data obtained for (F_8TPP)Fe^{II},[40] which show a single pyrrole resonance (due to the symmetry of the F_8TPP porphyrin macrocycle), and whose chemical shift is contingent upon the solvent-dependent spin state of the ferrous heme (Table 1): (i) in noncoordinating solvents (i.e., CH_2Cl_2, toluene), (F_8TPP)Fe^{II} has a pyrrole resonance at δ 4.9 ppm, indicative of a four-coordinate $S = 1$ spin system;[30,40,51−53] (ii) in weakly to moderately coordinating solvents (acetone, THF), (F_8TPP)-Fe^{II} has a downfield-shifted pyrrole resonance (δ 48−56 ppm), which has been previously shown to be consistent with either a five- or six-coordinate $S = 2$ ferrous heme; (iii) in MeCN solvent, (F_8TPP)Fe^{II} shows a pyrrole resonance at δ 28 ppm, which has been ascribed to a signal representing an equilibrium mixture of five-coordinate high-spin (one axial-bound MeCN ligand) and six-coordinate low-spin (bis-MeCN axial ligation) species. This equilibrium can be perturbed, as demonstrated through variable-temperature ^{1}H NMR spectroscopic studies, which show that the formation of the six-coordinate low-spin species is favored at lower temperature, while the five-coordinate high-spin heme is preferred at higher temperature. These differences between (^{6}L)Fe^{II} (**1**) and (F_8TPP)Fe^{II} imply the consistent presence of an axial base ligand in **1**, thus giving rise to a five-coordinate high-spin ferrous heme even when no exogenous axial ligand (i.e., no coordinated solvent ligand, as is the case for CH_2Cl_2) is present. We thus conclude that a pyridyl arm is coordinated to the ferrous heme in all solvents except THF (vide infra), Scheme 1.

Supporting evidence for the ferrous-heme pyridyl arm coordination comes from the observation in the ^{1}H NMR spectra of (^{6}L)Fe^{II} (**1**) of non-pyrrolic resonances appearing both downfied ($\sim\delta$ 20−24 ppm) and upfield ($\sim\delta$ −8 to −13 ppm) in all solvents except THF (Figure 1). These paramagnetically shifted resonances are not observed in (F_8TPP)-Fe^{II},[40] and we have therefore assigned these peaks in **1** to pyridyl-H resonances arising from the binding of a pyridyl arm (from the Cu-free TMPA chelate) to the high-spin

Scheme 1

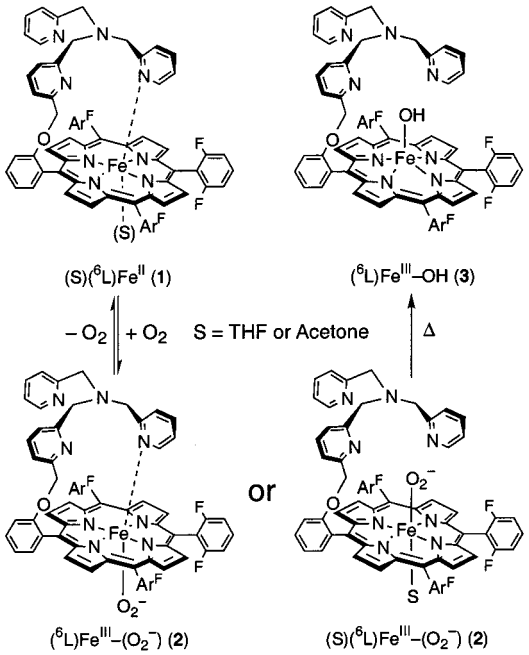

ferrous heme. While their unambiguous assignment was not confirmed by deuteration or methylation, the ∼20 ppm resonance can be attributed to the H_{para} proton of the pyridyl arm, while the upfield resonance (ca. −10 ppm) can be ascribed to the CH_2-pyridyl methylene linker.[44,45,54] An examination of five-coordinate Fe(II) model hemes (synthetic analogues of cytochrome *c* oxidase, deoxyhemoglobin/deoxymyoglobin, cytochrome P-450 monooxygenase and chloroperoxidase) in the literature reveals similar patterns of paramagnetically shifted resonances corresponding to axially bound or heme-bound exogenous ligands (substituted imidazoles,[47] pyridines,[34,49,50] mercaptides,[55,56] *N*-alkyl or -aryl porphyrins,[57] and nitrene complexes[44]).

For (^{6}L)Fe^{II} (**1**), these up- and downfield-shifted pyridyl-H resonances appear in CH_2Cl_2 (noncoordinating), acetone (moderately coordinating), and MeCN (moderately coordinating) solvents, but not in tetrahydrofuran solvent. While the expectation of pyridyl arm coordination to the heme in lieu of solvent is reasonable for the noncoordinating CH_2-Cl_2 solvent, we suggest the preference of the heme to bind the pyridyl arm over the moderately coordinating MeCN and acetone solvents is due (in part) to the intramolecular binding of the covalently attached TMPA-chelate pyridyl arms, despite the solvents being present in large excess. While the lack of shifted pyridyl-H resonances in the weak-field THF solvent appears to be an anomaly, it has been previously shown[58] that (F_8TPP)Fe^{II} exists as a bis(THF) complex (six-

(46) Collman, J. P.; Brauman, J. I.; Doxsee, K. M.; Halbert, T. R.; Bunnenberg, E.; Linder, R. E.; La Mar, G. N.; Del Gaudio, J.; Lang, G.; Spartalian, K. *J. Am. Chem. Soc.* **1980**, *102*, 4182−4192.
(47) Collman, J. P.; Brauman, J. I.; Collins, T. J.; Iverson, B. L.; Lang, G.; Pettman, R. B.; Sessler, J. L.; Walters, M. A. *J. Am. Chem. Soc.* **1983**, *105*, 3038−3052.
(48) Tsuchida, E.; Komatsu, T.; Arai, K.; Nishide, H. *J. Chem. Soc., Dalton Trans.* **1993**, 2465−2469.
(49) Momenteau, M.; Loock, B. *J. Mol. Catal.* **1980**, *7*, 315−320.
(50) Momenteau, M.; Mispelter, J.; Loock, B.; Lhoste, J.-M. *J. Chem. Soc., Perkin Trans. 1* **1985**, 221−231.
(51) Goff, H.; La Mar, G. N.; Reed, C. A. *J. Am. Chem. Soc.* **1977**, *99*, 3641−3646.
(52) Mispelter, J.; Momenteau, M.; Lhoste, J.-M. *Mol. Phys.* **1977**, *33*, 1715.
(53) McGarvey, B. R. *Inorg. Chem.* **1988**, *27*, 4691.
(54) While resonances ascribed to the H_{ortho} proton (80−140 ppm) of coordinated pyridyl groups have been previously reported (see refs 44−45 and references therein), we were unable to detect such a resonance for **1**, possibly because of the limited spectral window (100 to −100 ppm) of the NMR instrument under our data collection parameters (see Experimental Section for details).
(55) Lukat, G.; Goff, H. M. *Biochim. Biophys. Acta* **1990**, *1037*, 351−359.
(56) Parmely, R. C.; Goff, H. M. *J. Inorg. Biochem.* **1980**, *12*, 269−280.
(57) Balch, A. L.; Chan, Y.-W.; La Mar, G. N.; Latos-Grazynski, L.; Renner, M. W. *Inorg. Chem.* **1985**, *24*, 1437.

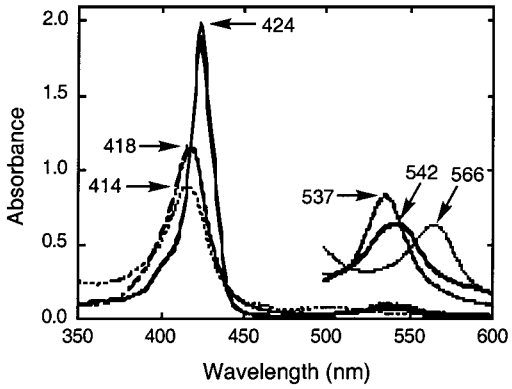

Figure 2. UV-vis spectra (THF, 193 K) upon reversible oxygenation of (^{6}L)Fe^{II} (**1**) (five oxygenation cycles shown): (−−) (^{6}L)Fe^{II} (**1**) {λ_{max} = 424 (Soret), 542 nm}, (- · -) (^{6}L)Fe^{III}−(O_2^-) (**2**) {λ_{max} = 418 (Soret), 537 nm}, (- - -) (^{6}L)Fe^{III}−OH (**3**) {λ_{max} = 414 (Soret), 566 nm}. See text for further explanation.

coordinate, high-spin) in this solvent. Thus, THF appears to be a stronger iron(II) ligand compared to acetone or acetonitrile, and its presence as the solvent precludes pyridyl arm coordination in (^{6}L)Fe^{II} (**1**) and the subsequent shifting of the pyridyl-H resonances outside the diamagnetic region.

The presence of the pyridyl arms available for iron ion binding in (^{6}L)Fe^{II} (**1**) has clear implications for dioxygen binding. Unlike the O_2-binding chemistry of (F_8TPP)Fe^{II} itself,[40] the formation of heme−superoxo species (with coordinated axial ligand solvent or pyridyl arm) should (and does) predominate over heme−peroxo−heme dinuclear complex generation in the oxygenation of (^{6}L)Fe^{II} (**1**), regardless of the choice of reaction solvent employed. This expectation is confirmed by the ^{2}H NMR study of the (^{6}L)-Fe^{II} (**1**)/O_2 reaction in various solvents, as described in a following section.

Dioxygen Binding to (^{6}L)Fe^{II} (1) in Tetrahydrofuran. Initial indications that (^{6}L)Fe^{II} (**1**) forms a dioxygen adduct came from low-temperature UV−vis spectroscopy (Figure 2). Bubbling O_2 through a solution of (^{6}L)Fe^{II} (**1**) {λ_{max} = 424 (Soret), 542 nm} in THF solvent at 193 K reveals the presence of a new species, formulated as the heme−superoxo complex (^{6}L)Fe^{III}−(O_2^-) (**2**) {λ_{max} = 418 (Soret), 537 nm}, which was found to be stable indefinitely at this temperature. While application of a simple vacuum to the solution was unable to reverse the dioxygen binding, direct bubbling of argon through the solution for 15 min at 193 K was sufficient to give back the reduced complex (^{6}L)Fe^{II} (**1**). This reversible cycling of dioxygen binding and removal can be performed at least five times without significant decomposition to the ultimate thermal decomposition product being observed, the ferric−hydroxy complex (^{6}L)Fe^{III}−OH (**3**) {λ_{max} = 414 (Soret), 566 nm} (Figure 2). Detection of dioxygen liberated from a solution of **2** (excess O_2 removed; THF, 193 K) by means of argon bubbling was confirmed by a qualitative alkaline pyrogallol test for dioxygen evolution (see Experimental Section), thereby confirming the formulation of **2** as a heme−O_2 adduct.

(58) Thompson, D. W.; Kretzer, R. M.; Lebeau, E. L.; Scaltrio, D.; Ghiladi, R. A.; Lam, K.-C.; Rheingold, A. L.; Meyer, G. J.; Karlin, K. D. Manuscript in preparation.

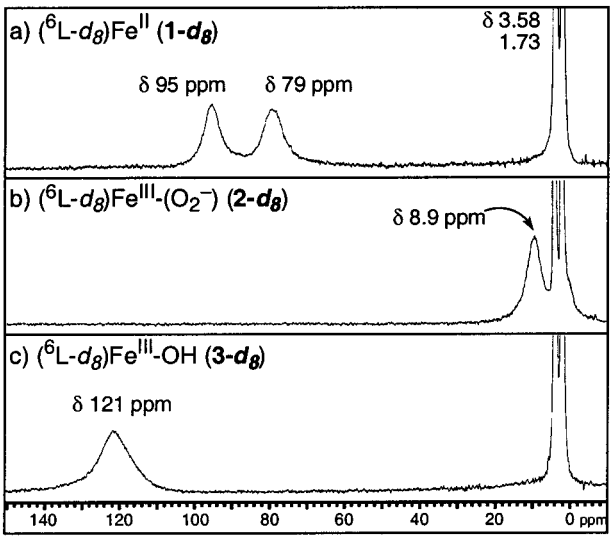

Figure 3. ^{2}H NMR spectra of the oxygenation reaction of (^{6}L-d_8)Fe^{II} (**1-d_8**) in THF solvent at 193 K. The strong signals at δ 3.58 and δ 1.73 ppm correspond to THF solvent. See text for further discussion.

Further characterization of the (^{6}L)Fe^{II} (**1**)/O_2 oxygenation reaction product in THF solvent comes from low-temperature ^{2}H NMR spectroscopy. The reduced complex (^{6}L-d_8)Fe^{II} (**1-d_8**) shows two pyrrole resonances (THF solvent, 193 K), δ 79 and δ 95 ppm (Figure 3a), contrasting to the room temperature observations discussed previously; a five-coordinate high-spin ferrous heme is still indicated.[43−45] There are two candidates for the ferrous heme's fifth axial ligand: a bound THF (solvent) ligand, or a bound pyridine from the tethered TMPA moiety, originating either inter- or intramolecularly. Previous work with the parent porphyrin complex, (F_8TPP)Fe^{II},[40] has shown downfield shifted pyrrole resonances at δ 93 ppm in THF solvent at 193 K. Furthermore, as is discussed later, (^{6}L-d_8)Fe^{II} (**1-d_8**) in CH_2Cl_2, a noncoordinating solvent, also shows a downfield shifted pyrrole resonance (due to a coordinated TMPA-pyridyl arm), but at δ 75 ppm (193 K). These results suggest that the δ 79 and δ 95 ppm pyrrole resonances for (^{6}L-d_8)Fe^{II} (**1-d_8**) {THF, 193 K} represent a mixture of species present. One species, with axially bound THF solvent to the ferrous heme, gives rise to the δ 95 ppm resonance, whereas the second species, with bound pyridine from the TMPA moiety, is responsible for the δ 79 ppm spectral feature.

Oxygenation of the reduced complex (^{6}L-d_8)Fe^{II} (**1-d_8**) in THF at 193 K shows an immediate shift in the pyrrole resonance to δ 8.9 ppm for (^{6}L-d_8)Fe^{III}−(O_2^-) (**2-d_8**) (Figure 3b). Upon warming the sample to room temperature for several hours to facilitate decomposition, followed by recooling, the pyrrole hydrogen resonance was found downfield shifted to δ 121 ppm (Figure 3c), consistent with an assignment to the previously characterized[41] high-spin ferric−hydroxy product, (^{6}L-d_8)Fe^{III}−OH (**3-d_8**). As can be seen by the $\delta_{pyrrole}$ values of selected heme−O_2 adducts listed in Table 2, the chemical shift of δ 8.9 ppm for the pyrrole resonances is indicative of a low-spin heme−superoxo complex, formulated as (^{6}L-d_8)Fe^{III}−(O_2^-) (**2**).[59] We have postulated that the sixth axial ligand present in **2** is either a bound THF solvent molecule or a coordinated pyridyl arm from the

Table 2. Pyrrole Chemical Shifts of Selected Heme−O_2 Adducts[a]

heme−O_2 adduct	$\delta_{pyrrole}$	solvent	temp (K)	ref
(^{6}L−d_8)Fe^{III}−(O_2^-) (**2**)	8.9	THF	193	*b*
(^{6}L−d_8)Fe^{III}−(O_2^-) (**2**)	8.9	acetone	193	*b*
(^{6}L−d_8)Fe^{III}−(O_2^-) (**2**)	9.3	CH_2Cl_2	193	*b*
(THF)(F_8TPP)Fe^{III}−(O_2^-)	8.9	THF	193	40
(acetone)(F_8TPP)Fe^{III}−(O_2^-)	8.9	acetone	193	40
(*N*-MeIm)(TMP)Fe^{III}−(O_2^-)	8.37	toluene-d_8	196	69
(TpivPP)Fe^{III}−(O_2^-)[c]	8.2	toluene-d_8	197	70
(T(2,4,6-MeO)$_3$PP)Fe^{III}−(O_2^-)[c]	9.0	CD_2Cl_2	198	70
(T(2,4,6-EtO)$_3$PP)Fe^{III}−(O_2^-)[c]	9.1	CD_2Cl_2	198	70
(T(3,4,5-MeO)$_3$PP)Fe^{III}−(O_2^-)[c]	9.8	toluene-d_8	198	70
[(F_8TPP)Fe^{III}]$_2$−(O_2^{2-})	17.5	CH_2Cl_2	193	40
[(TMP)Fe^{III}]$_2$−(O_2^{2-})	17.7, 19.0	toluene-d_8	203, 243	69
[(TPP)Fe^{III}]$_2$−(O_2^{2-})	16.0	toluene-d_8	193	71
[(TpivPP)Fe^{III}]$_2$−(O_2^{2-})	16.6	toluene-d_8	248	70
[(TmTP)Fe^{III}]$_2$−(O_2^{2-})	16.2	toluene-d_8	193	71
[(DPDMe)Fe^{III}]$_2$−(O_2^{2-})	19.2	toluene-d_8	199	71
[(T(3,4,5-MeO)$_3$PP)Fe^{III}]$_2$−(O_2^{2-})	16.8	toluene-d_8	243	70

[a] F_8TPP = *meso*-tetrakis(2,6-difluorophenyl)porphyrin; TMP = *meso*-tetramesitylporphyrin; TpivPP = *meso*-tetrakis(α,α,α,α-*o*-pivalamidophenyl)porphyrin; T(2,4,6-MeO)$_3$PP = *meso*-tetrakis(2,4,6-trimethoxyphenyl)porphyrin; T(2,4,6-EtO)$_3$PP = *meso*-tetrakis(2,4,6-triethoxyphenyl)-porphyrin; T(3,4,5-MeO)$_3$PP = *meso*-tetrakis(3,4,5-trimethoxyphenyl)-porphyrin; TPP = *meso*-tetraphenylporphyrin; TmTP = *meso*-tetra-*m*-tolylporphyrin; DPDMe = deuterioporphyrin IX dimethyl ester; *N*-MeIm = *N*-methylimidazole. [b] This work. [c] Five-coordinate, diamagnetic complex due to lack of a suitable axial base.

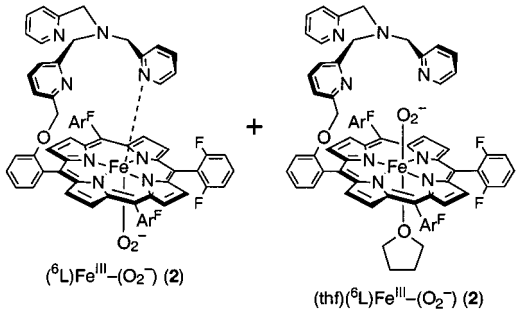

Figure 4. Two possible modes of sixth axial ligand coordination in (^{6}L)-Fe^{III}−(O_2^-) (**2**) in THF solvent.

tethered TMPA moiety, with the NMR spectroscopic data being unable to differentiate between these two possibilites (Figure 4).

In acetone solvent, similar chemistry to that of THF is observed and is discussed in detail in the Supporting Information. Dioxygen binding and pyridyl arm coordination to the heme−superoxo complex **2** will be discussed below for the case of CH_2Cl_2 as reaction solvent.

Dioxygen Binding to (^{6}L)Fe^{II} (1) in Methylene Chloride. As was the case for THF solvent, initial indications of a dioxygen adduct of (^{6}L)Fe^{II} (**1**) in methylene chloride solvent came from low-temperature UV−vis spectroscopy (Figure 5). Addition of dioxygen to a solution of (^{6}L)Fe^{II} (**1**) {λ_{max} = 433 (Soret), 529 (sh), 559 nm} in CH_2Cl_2 solvent at 193 K reveals the presence of a stable species, formulated as the heme−superoxo complex (^{6}L)Fe^{III}−(O_2^-) (**2**), with spectral features at 422 (Soret) and 542 nm. While application of a simple vacuum to the solution was unable to reverse the

(59) Initial resonance Raman spectroscopic investigations (with Prof. Pierre Moënne-Loccoz, OGI School of Science and Engineering at OHSU, Beaverton, OR) on (^{6}L)Fe^{III}−(O_2^-) (**2**) have revealed a ν(O−O) = 1176 cm^{-1}, which shifts upon substitution with $^{18}O_2$ by −64 cm^{-1}. Further studies are in progress.

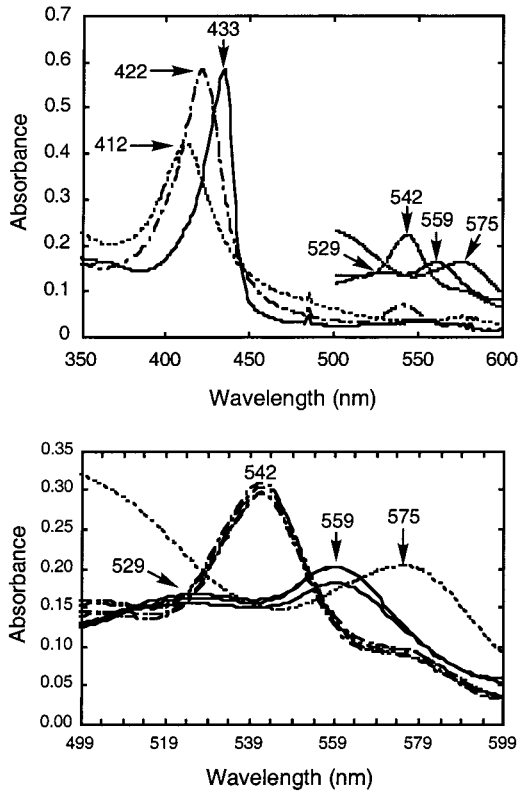

Figure 5. UV−vis spectra (CH_2Cl_2, 193 K) upon reversible oxygenation of (^{6}L)Fe^{II} (**1**) (top) and three cycles of reversible O_2-binding spectra (α band region, bottom): (−−) (^{6}L)Fe^{II} (**1**) {λ_{max} = 433 (Soret), 529 (sh), 559 nm}, (- · -) (^{6}L)Fe^{III}−(O_2^-) (**2**) {λ_{max} = 422 (Soret), 542 nm}, (- - -) (^{6}L)Fe^{III}−OH (**3**) {λ_{max} = 412 (Soret), 575 nm}. See text for further explanation.

dioxygen binding, direct bubbling of argon through the chilled solution for 15 min was sufficient to give back the reduced complex (^{6}L)Fe^{II} (**1**). This reversible cycling of dioxygen binding and removal can be performed only two or three times before significant decomposition to the ferric−hydroxy complex, (^{6}L)Fe^{III}−OH (**3**) {λ_{max} = 412 (Soret), 575 nm}, is observed (Figure 5). Furthermore, while heme−superoxo complex **2** was stable indefinitely at low temperature, it ultimately decomposes (thermally) to (^{6}L)Fe^{III}−OH (**3**). Because of the presence of the tethered arms with pyridyl donors which are present in ^{6}L, these results differ from the dioxygen reactivity of (F_8TPP)Fe^{II} in CH_2Cl_2 solvent,[40] which irreversibly forms a heme−peroxo−heme dinuclear complex (F_8TPP)Fe^{III}−(O_2^{2-})−Fe^{III}(F_8TPP) {UV−vis: 414 (Soret), 536 nm}.

Additional characterization of the (^{6}L)Fe^{II} (**1**)/O_2 oxygenation reaction product in methylene chloride solvent came from variable-temperature ^{2}H NMR spectroscopy (Figure 6). Contrasting again with the behavior of (F_8TPP)Fe^{II} in CH_2Cl_2 solvent (vide supra),[40] the pyrrole resonances of (^{6}L-d_8)-Fe^{II} (**1**-d_8) in CH_2Cl_2 at room temperature appear downfield between δ 43 and 46 ppm (Figure 6a), indicative of a high-spin five-coordinate ferrous heme. In this case, without a suitable coordinating solvent to bind to the heme, the fifth axial ligand can be ascribed to the binding of a pyridyl arm of the TMPA tether to the heme, either through an intra- or intermolecular fashion (vida supra). Upon cooling to 193 K,

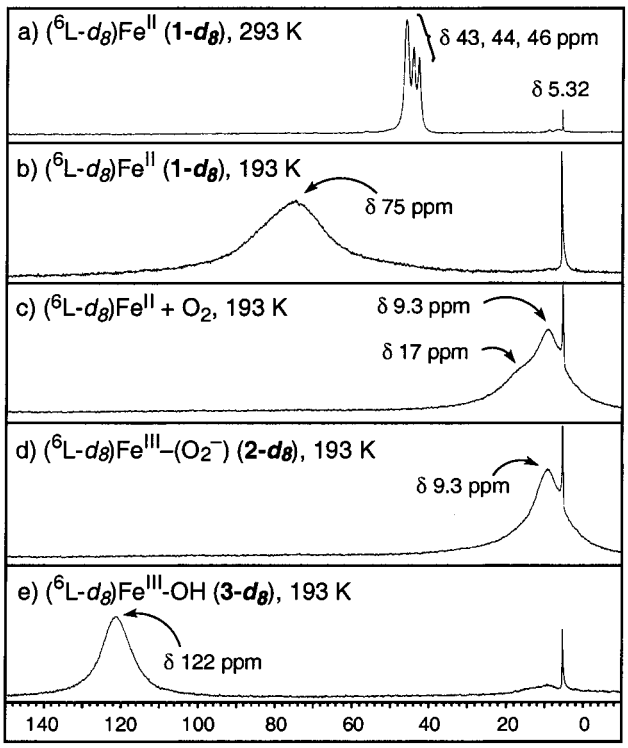

Figure 6. ^{2}H NMR spectra of the oxygenation reaction of (^{6}L-d_8)Fe^{II} (**1-d_8**) in CH_2Cl_2 solvent at 193 K. The strong resonance at δ 5.32 ppm is due to the methylene chloride solvent. See text for further discussion.

the pyrrole resonances can be found further downfield at δ 75 ppm (Figure 6b), also indicative of a high-spin five-coordinate ferrous heme.

Oxygenation of the (^{6}L-d_8)Fe^{II} (**1-d_8**) complex in CH_2Cl_2 at 193 K shows a mixture of dioxygen adducts formed by NMR spectroscopy. Initially (within 15 min), two resonances are observed (Figure 6c): a major peak {δ 9.3 ppm} which can be attributed to a low-spin six-coordinate heme−superoxo complex, (^{6}L-d_8)Fe^{III}−(O_2^-) (**2**), and a broad shoulder at δ 17 ppm, which we ascribe to the formation of a heme−peroxo−heme dimer complex, (^{6}L-d_8)Fe^{III}−(O_2^{2-})−Fe^{III}(^{6}L-d_8), with noncoordinated pyridine arms. As mentioned, heme−peroxo−heme intermolecular dimers (Table 2) have been previously observed for the oxygenation of (F_8TPP)Fe^{II} in noncoordinating solvents, yielding (F_8TPP)Fe^{III}−(O_2^{2-})−Fe^{III}(F_8TPP) {$\delta_{pyrrole}$ = 17.5 ppm, 193 K, CH_2Cl_2}.[40] While the (^{6}L-d_8)Fe^{III}−(O_2^{2-})-Fe^{III}(^{6}L-d_8) dimer forms initially as a minor oxygenation product, it is thermally unstable at 223 K and immediately rearranges to form only the heme−superoxo complex (^{6}L-d_8)Fe^{III}−(O_2^-) (**2**), with a single pyrrole hydrogen resonance appearing at δ 9.3 ppm (Figure 6d). Upon warming to room temperature to promote decomposition, followed by recooling to 193 K, the spectrum of the high-spin ferric−hydroxy product, (^{6}L-d_8)Fe^{III}−OH (**3-d_8**) {δ 122 ppm}, was observed (Figure 6e). Given that the formation of a low-spin heme−superoxo complex (^{6}L-d_8)Fe^{III}−(O_2^-) (**2**) occurs here in the noncoordinating CH_2Cl_2 solvent, it is possible to ascribe a sixth axial ligand in this dioxygen adduct to a coordinated pyridyl arm of the TMPA unit.

While it is not possible to assign the pyridyl arm coordination as a purely intramolecular one, the observation of a low-spin heme−superoxo complex, such as (^{6}L)Fe^{III}−(O_2^-) (**2**), indicates that a covalently attached pyridine at the 2-position is capable of acting as an axial base in these types of oxygenation reactions. Heme−superoxo complexes of the form (B)PFe^{III}−(O_2^-), where B represents a substituted imidazole axial base ligand, have been previously studied in the literature.[7,46,47,60−64] Although the kinetics and thermodynamics of O_2-binding to five-coordinate high-spin hemes are more favorable for 1-methylimidazole (as an R state model of hemoglobin) versus the more sterically hindered 1,2-dimethylimidazole (as a model for the T state of hemoglobin), both axial base situations yield characterizable heme−superoxo complexes. We speculate that the binding of the 2-substituted pyridyl arm in (^{6}L)Fe^{II} (**1**) may be very similar to the binding of 1,2-dimethylimidazole to other heme systems, with the ferric ion slightly pulled out of the plane of the porphyrin macrocycle toward the axial base (i.e., T state model of hemoglobin).

Conclusions

Following the techniques which have been previously utilized for analyzing such systems, multinuclear (^{1}H and ^{2}H) NMR and UV−vis spectroscopies have been employed to investigate the behavior of (^{6}L)Fe^{II} (**1**) and its low-temperature stable dioxygen adducts in a variety of solvents. ^{1}H NMR spectroscopy of (^{6}L)Fe^{II} (**1**) in a number of solvents ranging in their coordination ability as axial ligands revealed the consistent presence of downfield-shifted pyrrole resonances, indicative of (^{6}L)Fe^{II} (**1**) possessing a solvent-independent five-coordinate high-spin ($S = 2$) ferrous heme. Furthermore, evidence of pyridyl arm coordination to the ferrous heme in several solvents was also suggested by the appearance of non-pyrrolic paramagnetically shifted (pyridyl-H or 2-pyridyl-CH_2) resonances in the ^{1}H NMR spectra.

This conclusion of pyridyl arm coordination present in (^{6}L)Fe^{II} (**1**) is also substantiated through comparisons of the dioxygen reactivity of (F_8TPP)Fe^{II} with **1** in both coordinating and noncoordinating solvents. Both complex **1** and (F_8TPP)Fe^{II} form six-coordinate low-spin ferric−superoxo complexes upon low-temperature oxygenation in coordinating solvent, as determined from their chemical shift of the β-pyrrole-H resonances. However, oxygenation of (^{6}L)Fe^{II} (**1**) yields predominantly heme−superoxo complex (^{6}L)Fe^{III}−(O_2^-) (**2**) {$\delta_{pyrrole}$ = 9.3 ppm} in CH_2Cl_2 (noncoordinating) solvent, whereas (F_8TPP)Fe^{II} forms μ-peroxo complex (F_8TPP)Fe^{III}−(O_2^{2-})−Fe^{III}(F_8TPP) {$\delta_{pyrrole}$ = 17.5 ppm} under identical conditions. There is an indication that (^{6}L)Fe^{III}−(O_2^{2-})−Fe^{III}(^{6}L) {$\delta_{pyrrole}$ = 17.0 ppm} is formed initially and in minor amounts at 193 K, but it immediately rearranges to (^{6}L)Fe^{III}−(O_2^-) (**2**) upon warming to 223 K. In light of

(60) Collman, J. P.; Brauman, J. I.; Doxsee, K. M.; Halbert, T. R.; Suslick, K. S. *Proc. Natl. Acad. Sci. U.S.A.* **1978**, *75*, 564−568.
(61) Collman, J. P.; Brauman, J. I.; Iverson, B. L.; Sessler, J.; Morris, R. M.; Gibson, Q. H. *J. Am. Chem. Soc.* **1983**, *105*, 3052−3064.
(62) Weschler, C. J.; Anderson, D. L.; Basolo, F. *J. Am. Chem. Soc.* **1975**, *97*, 6707−6713.
(63) Linard, J. E.; Ellis, P. E., Jr.; Budge, J. R.; Jones, R. D.; Basolo, F. *J. Am. Chem. Soc.* **1980**, *102*, 1896−1904.
(64) David, S.; James, B. R.; Dolphin, D.; Traylor, T. G.; Lopez, M. A. *J. Am. Chem. Soc.* **1994**, *116*, 6−14.

the lack of a solvent-based axial ligand in methylene chloride, we suggest that a pyridyl arm of the ^{6}L ligand is coordinated to the ferric heme of (^{6}L)Fe^{III}−(O_2^-) (**2**), thereby providing a sixth axial ligand to stabilize the dioxygen adduct.

While the work presented here has focused primarily on the O_2-reactivity of (^{6}L)Fe^{II} (**1**), the conclusions based upon this work, and that of the (F_8TPP)Fe^{II} system as well, provide the basis for understanding the dioxygen binding and reduction chemistry of similar heme−Cu systems, such as [(^{6}L)-Fe^{II}Cu^{I}]$^+$.[33,42] With respect to either tethered systems (based upon the ^{6}L ligand or similar architecture) or untethered systems (employing the F_8TPPH_2 porphyrin), the formation of heme−superoxo complexes as precursors to heme−Cu/O_2 heterobinuclear dioxygen adducts is viable. Moreover, the ability of a 2-substituted pyridyl arm to bind to a heme−superoxo complex is significant, given that a similar type of 2-substituted pyridine (as a covalently tethered axial base ligand) is thought to coordinate to the heme−peroxo−Cu complex [(^{4}L)Fe^{III}−(O_2^{2-})Cu^{II}]$^+$ [34] (see introductory diagram).

Experimental Section

Materials and Methods. Reagents and solvents were purchased from commercial sources and were of reagent grade quality. All solvents were distilled under Ar prior to use: dichloromethane (CH_2Cl_2) was distilled directly from CaH_2, acetone was distilled over Drierite, and tetrahydrofurn was distilled from Na/benzophenone. Preparation and handling of air-sensitive materials was carried out under an argon atmosphere using standard Schlenk techniques. Solvents and solutions were deoxygenated by either repeated freeze−pump−thaw cycles, or by bubbling of argon (20−30 min) directly through the solution. Solid samples were stored and transferred, and samples for NMR spectroscopy were prepared, in an MBraun LabMaster 130 inert atmosphere (<1 ppm O_2, <1 ppm H_2O) glovebox under nitrogen atmosphere. Dioxygen used for O_2-adduct formation was ultrapure grade (99.994%), obtained from WSC (Baltimore, MD).

NMR spectra were measured on a Varian NMR instrument at 400 MHz (^{1}H) or 61 MHz (^{2}H). All spectra were recorded in 5-mm o.d. NMR tubes, and chemical shifts were reported as δ values downfield from an internal standard of Me_4Si (^{1}H NMR), or as δ values calibrated to natural abundance deuterium solvent peaks with shifts referenced downfield from TMS (^{2}H NMR). Low-temperature UV−vis spectral studies were carried out with a Hewlett-Packard 8453 diode array spectrometer equipped with HPChemstation software. The spectrometer was equipped with a variable-temperature Dewar and cuvette assembly as described elsewhere.[65,66]

Variable Temperature NMR Studies. Both deuterated and undeuterated solvents were distilled and degassed prior to use. In the glovebox, typically a solution containing 10−20 mg of (^{6}L)-Fe^{II} (**1**) in 1 mL of solvent (deuterated solvent for ^{1}H NMR spectra, undeuterated solvent for ^{2}H NMR) was prepared and transferred to a 5 mm o.d. ultrathin wall NMR tube with a screw-cap septum top (Wilmad Glass). ^{1}H and ^{2}H NMR spectra were recorded at room temperature before cooling to the desired temperature. Addition of dioxygen at low temperature was carried out in the following manner: the NMR tube was removed from the spectrometer, placed in either a dry ice/acetone bath or directly into dry ice, and using a Hamilton gastight syringe, excess O_2 was bubbled directly through the solution by piercing the septum cap with a long syringe needle. Typical spectra were recorded at 100 kHz spectral width with no delay between 90° pulses of 7.2 μs or 17.5 μs for ^{1}H or ^{2}H NMR spectra, respectively. Referencing/calibration of the spectra was performed as described previously for each given temperature, and shift values are reported at the stated temperature; for ^{1}H and ^{2}H NMR, those resonances positive to TMS are downfield, and those negative are upfield.

UV−Vis Spectroscopic Studies and Reversible O_2-Binding. In the glovebox, a solution of **1** in the desired solvent was prepared and transferred to a modified low-temperature cuvette assembly equipped with a Schlenk-type sidearm.[65,66] After cooling to 193 K, generation of the dioxygen adducts was carried out by bubbling the chilled solution with dioxygen. Removal of excess O_2 was performed by simple application of vacuum at 193 K. Reversible binding was carried out by bubbling the solution with argon using a syringe needle at 193 K.

Alkaline Pyrogallol Test for Dioxygen Evolution. These experiments were adapted from methods previously described.[66−68] In the glovebox, a solution of **1** (20 mg) in THF (∼15 mL) was prepared and transferred to a Schlenk flask capped with a rubber septum. Bubbling of dioxygen via syringe needle at 193 K afforded the desired dioxygen adduct, (^{6}L)Fe^{III}−(O_2^-) (**2**). Removal of excess O_2 was performed with multiple freeze−pump−thaw cycles (thawing temperature was 193 K), yielding a solution whose only source of dioxygen was the heme−O_2 adduct.

To a special Schlenk flask modified with a quartz cuvette and equipped with a stir bar was added 4.0 g of pyrogallol and 25 mL of deoxygenated 50% KOH (aq) solution under Ar. The alkaline pyrogallol solution was a faint beige color, and its UV−vis spectrum was recorded (λ_{400nm} = ∼0.04−0.05). Using a syringe needle, argon was bubbled directly through the solution of **2** at 193 K, liberating O_2 into the headspace of the Schlenk flask, which was then passed through a cannula and bubbled directly into the stirring alkaline pyrogallol solution, whose color began to darken after 1 min. After approximately 20 min, the pyrogallol solution ceased becoming darker, and its spectrum was re-recorded (λ_{400nm} = ∼0.25−0.27). This process was repeated under identical conditions but without **1** present as a control, and showed no significant increase in absorbance (λ_{400nm} = ∼0.05−0.06).

Acknowledgment. We are grateful to the National Institutes of Health (K.D.K., Grants GM28962 and GM60353) for support of this research.

Supporting Information Available: Discussion of dioxygen reactivity of (^{6}L)Fe^{II} (**1**) in acetone solvent {UV−vis (Figure S1) and ^{2}H NMR (Figure S2) spectroscopic characterization} yielding the heme−superoxo complex (^{6}L)Fe^{III}−(O_2^-) (**2**). This material is available free of charge via the Internet at http://pubs.acs.org.

IC0103547

(65) Karlin, K. D.; Cruse, R. W.; Gultneh, Y.; Farooq, A.; Hayes, J. C.; Zubieta, J. *J. Am. Chem. Soc.* **1987**, *109*, 2668−2679.
(66) Karlin, K. D.; Haka, M. S.; Cruse, R. W.; Meyer, G. J.; Farooq, A.; Gultneh, Y.; Hayes, J. C.; Zubieta, J. *J. Am. Chem. Soc.* **1988**, *110*, 1196−1207.
(67) Wei, N.; Murthy, N. N.; Chen, Q.; Zubieta, J.; Karlin, K. D. *Inorg. Chem.* **1994**, *33*, 1953−1965.
(68) A quantitative methodology will be described elsewhere. See ref 42.
(69) Balch, A. L.; Chan, Y.-W.; Cheng, R.-J.; La Mar, G. N.; Latos-Grazynski, L.; Renner, M. W. *J. Am. Chem. Soc.* **1984**, *106*, 7779−7785.
(70) Latos-Grazynski, L.; Cheng, R.-J.; La Mar, G. N.; Balch, A. L. *J. Am. Chem. Soc.* **1982**, *104*, 5992−6000.
(71) Chin, D.-H.; La Mar, G. N.; Balch, A. L. *J. Am. Chem. Soc.* **1980**, *102*, 4344−4350.